electronics

MDPI

Supplementary Material

Comparative Analysis of Thermal Properties in Molybdenum Substrate to Silicon and Glass for a System on Foil Integration

Tzu-Jung Huang[1], Tobias Kiebala[1], Paul Suflita[1], Chad Moore[2], Graeme Housser[2], Shane McMahon[2], and Ivan Puchades[1,*]

[1] Department of Microsystems Engineering, Rochester Institute of Technology, Rochester, NY 14623 USA; txh9958@rit.edu (T-J.H.); tmk9592@rit.edu (T.K.); ps8762@rit.edu (P.S.)

[2] Lux Semiconductors, Albany, NY 12203 USA; cmoore@luxsemiconductors.com (C.M.); ghousser@luxsemiconductors.com (G.H.); smcmahon@luxsemiconductors.com (S.M.)

* Correspondence: ivan.puchades@rit.edu; Tel.: +1-585-475-7294

Figure S1 shows microscope image of fabricated test structures, R_{heat} and a pair of R_{sense} resistors on **(a)**molybdenum **(b)**silicon **(c)**fused silica glass substrates. Streaks and crevasse from molybdenum substrate surface polishing can be observed in **Figure S1(a)**.

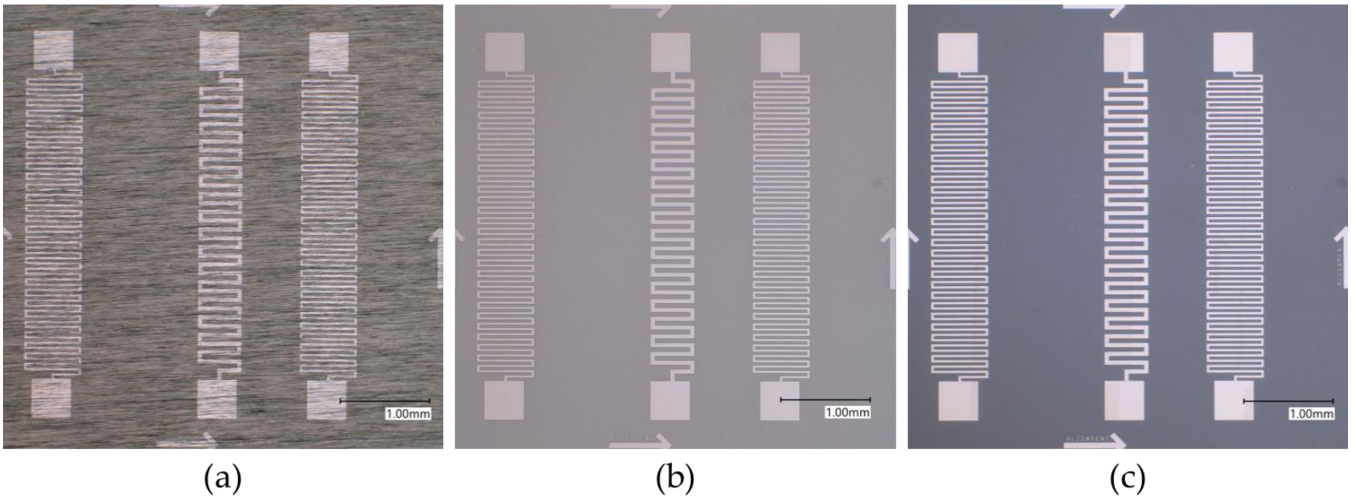

Figure S1. Microscope image of test structures on **(a)** molybdenum **(b)** silicon and **(c)** fused silica glass substrates

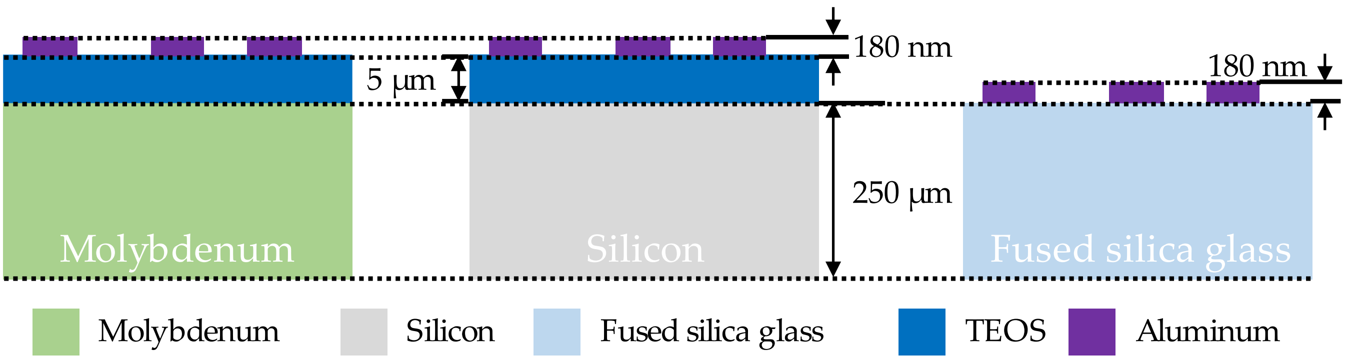

Figure S2. Illustrative cross-sectional depiction of fabricated test structures and its thin film heating and sense resistor on **(a)** molybdenum, **(b)** silicon and **(c)** fused silica glass substrates

Figure S3 illustrates thermal imaging of **(a)** molybdenum **(b)** silicon and **(c)** fused silica glass with Rheat power at 0 W, 1 W, 2 W, and 2.7 W. It can be observed that as progressing from 0 W to 2.7 W power applied, molybdenum substrate demonstrates its great thermal conductivity characteristics to spread out the heat when compared to silicon and especially fused silica glass substrates. Fused silica glass substrate has the worst thermal management parameters on paper and has been illustrated in experimental analysis as well. All the heat generated remained in the same spot with max temperature peaking to 166.0 °C at 2.7 W when compared to 40.3 and 40.9 °C for molybdenum and silicon substrates under the same power from Rheat.

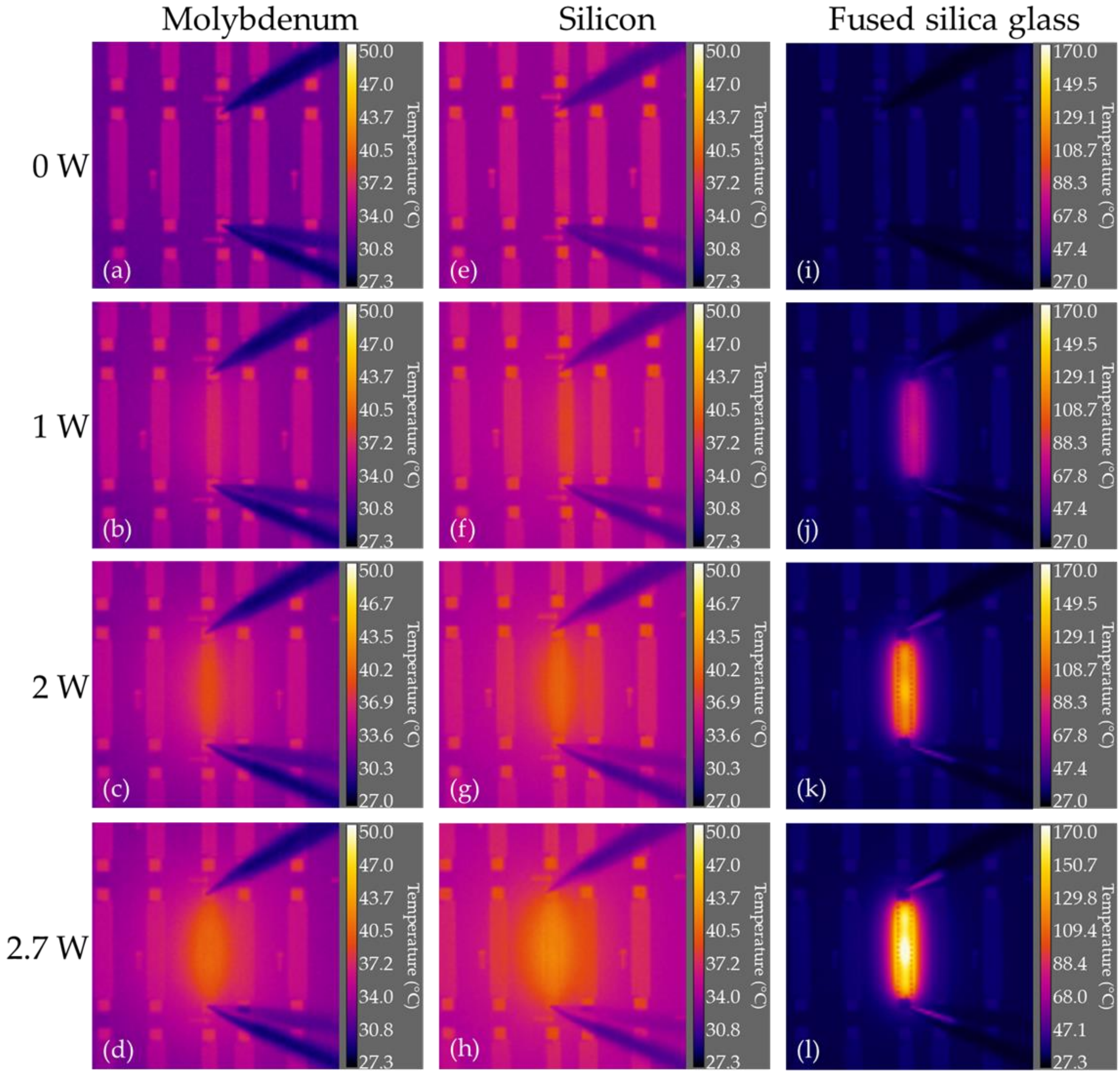

Figure S3. Static temperature measurement with FLIR AX5 thermal camera for **(a)-(d)** molybdenum, **(e)-(h)** silicon, and **(i)-(l)** fused silica glass substrates with 0 W, 1 W, 2 W and 2.7 W power from heating resistor (Rheat)

COMSOL Multiphysics was used to simulate a simplified heated structure. In the case of modeling and simulating this structure, the model wizard was first used to add all necessary modules. A 3D model should be selected, followed by the Heat Transfer in Solids and Events modules being added to the physics interface, allowing for accurate heat transfer and custom on/off pulsing to occur, respectively. For use in the analysis of a singular heat pulse, rather than repeated frequency pulse, a Time Dependent study was performed.

The geometry created to represent the heated structure is composed of three stacked components: the substrate, oxide layer, and metal heating element on top. The substrate is a block feature with dimensions of 10 mm x 10 mm x 250 μm (L x W x H). The oxide layer is a block feature with dimensions of 10 mm x 10 mm x 5 μm. The heating element is a block feature with dimensions of 4 mm x 0.5 mm x 180 nm located directly in the top-center of the substrate-oxide stack. These dimensions are intended to replicate the feature dimensions fabricated on the wafers tested.

A bill of materials is then added to the overall component, including materials to be tested for each of the features. Substrate materials include silicon, molybdenum, and fused silica; oxide layer materials include SiO_2; and heating element materials include aluminum. Each of these materials is then assigned to their respective features, relative to each test parameter. It is important to note that for any tests where the substrate used is fused silica glass, the SiO_2 oxide layer should disabled from the geometry and the heating element should be shifted to sit atop the substrate alone. This is due to the real borosilicate wafers tested being composed of a single material throughout.

Heat transfer functions are then introduced to the system, beginning with the initial and boundary conditions. The initial temperature condition of the entire domain is adjusted to 298 K, to reflect room temperature of the test conditions, implying that the device and ambient surroundings all begin at this temperature. Additionally, a constant temperature boundary condition of 298 K is applied to the bottom surface of the substrate in the model. This is intended to act as an artificial heat sink for the model, such that the data will reflect the heat transfer of a chip or wafer that is packaged on a heat sink or tested on top of a chuck, in the case of this paper. For the scope of this project, surface-to-ambient radiation will be ignored due to its minimal impact on the overall heat transfer system, whereas thermal conduction through the substrate governs the overall thermal management. Consequently,

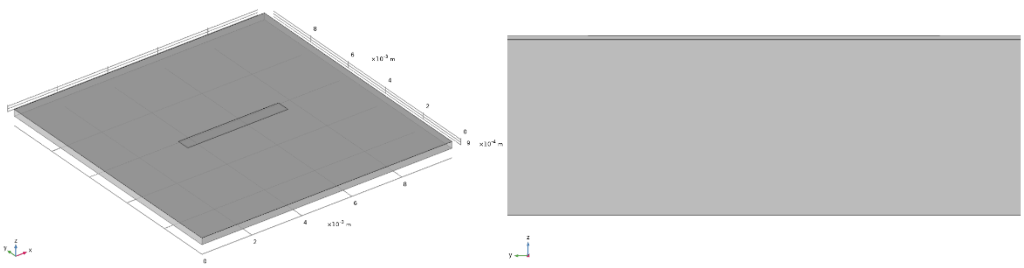

Figure S4. 3D isometric and 2D cross-sectional views of test structures modeled in component thickness correspond to dimensions referenced in **Figure 3**

The heat source is then added to the heat transfer section. Within the heat source settings, the heating element geometry should be assigned as the heat source. Then, the heat source requires a user defined heat flux density in W/m^3, which is simply the chosen power divided by the total volume of the heat structure. In this analysis, power values that are to be tested include 1, 2, and 2.7 W to be able to relate to experimental data collected. When the heat source is established, a specific heat pulse is chosen, typical pulse shapes can include square waves, sine waves, and many other variances of these. In this study, we focus on the application of a half-sine wave pulse to reflect the experimental methods. The half-sine pulse is a time dependent fun where the positive half of the sine wave is applied, but the negative half of a sine wave period is neglected, resorting to 0. Thus, the heat transfer that occurs at any given point within the model with respect to the applied heat flux, boundary conditions, and pulse time is defined by:

$$Q + Q_{ted} = \rho C_p u \cdot \nabla T + \nabla \cdot q \qquad \textbf{(S1)}$$

When finalizing the model prior to computing results, a mesh is built based on the existing geometry. The mesh utilized in this effort is composed of free-tetrahedrons whereby a physics-controlled mesh is built at the normal scale. This is acceptable as the tetrahedra are automatically shrunk to the minimum element sizing throughout the various geometries, optimizing the computing time while maintaining accurate simulation physics. By doing this, the results achieved are almost identical to the results achieved at a user-controlled finer mesh, but at a fraction of the computing time.

Subsequently, the model is then run with the purpose of performing parametric sweeps, where variables are changed, to collect data exemplifying the heat transfer performance of different substrate materials, at both a 2D and 3D level. Simulation results and imaging can thus characterize the respective maximum operating temperature and effective heat dissipation within these heated structures.

Figure S5 depicts simulation and experimental measured peak temperatures of the heat resistors superimposed to demonstrate that the simulated insulated response is more agreeable with the experimental data than the ideal simulation. The lack of a steady-state response in both sets of results confirms the absence of an ideal thermal connection to the heat sink. Though this study may be focused on the short-term thermal responses of specific pulses, however, the purpose of this is to emulate real-world device applications while also using short-term thermal responses to characterize heat dissipation over longer periods of time. Overall, a resistor or real-world device with an ideal heat sink would experience a steady-state response, such that the heat produced and dissipated throughout many cycles would reach a consistent maximum operating temperature. An ideal example of this can be seen in Figure 16 whereby maximum operating temperatures do not exceed the steady-state limit despite increasing pulse durations.

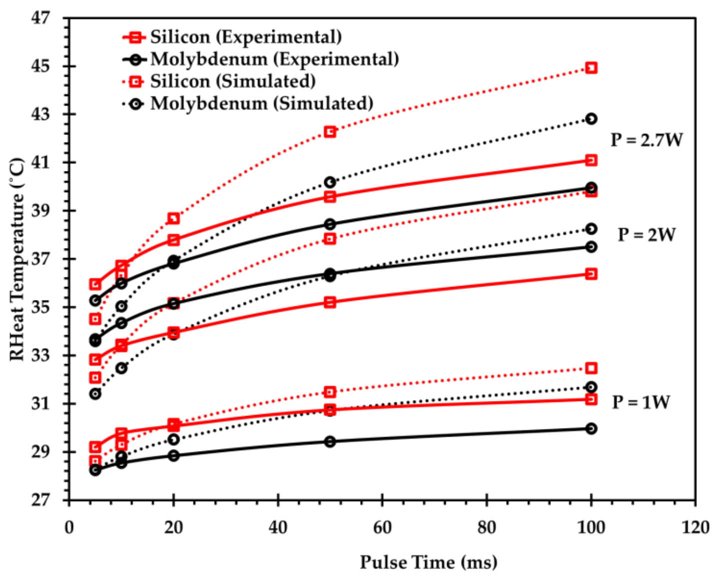

Figure S5. Superimposed simulation (dotted line) and experimental (solid line) measured peak temperature.